



Published in final edited form as:

Environ Sci Technol. 2013 November 5; 47(21): 12496–12504. doi:10.1021/es403146c.

Soy Biodiesel and Petrodiesel Emissions Differ in Size, Chemical Composition and Stimulation of Inflammatory Responses in Cells and Animals

Naomi K. Fukagawa^{1,*}, Muyao Li¹, Matthew E. Poynter¹, Brian C. Palmer¹, Erin Parker¹, John Kasumba², and Britt A. Holmén²

¹Department of Medicine, University of Vermont, Burlington, VT 05405

²School of Engineering, University of Vermont, Burlington, VT 05405

Abstract

Debate about the biological effects of biodiesel exhaust emissions exists due to variation in methods of exhaust generation and biological models used to assess responses. Because studies in cells do not necessarily reflect the integrated response of a whole animal, experiments were conducted in two human cell lines representing bronchial epithelial cells and macrophages and female mice using identical particle suspensions of raw exhaust generated by a Volkswagen light-duty diesel engine using petrodiesel (B0) and a biodiesel blend (B20: 20% soy biodiesel/80% B0 by volume). Tailpipe particle emissions measurement showed B0 generated two times more particle mass, larger ultrafine particle number distribution modes, and particles of more nonpolar organic composition than the B20 fuel. Biological assays (inflammatory mediators, oxidative stress biomarkers) demonstrated that particulate matter (PM) generated by combustion of the two fuels induced different responses in *in vitro* and *in vivo* models. Concentrations of inflammatory mediators (Interleukin-6, IL-6; Interferon-gamma-induced Protein 10, IP-10; Granulocyte-stimulating factor, G-CSF) in the medium of B20-treated cells and in bronchoalveolar lavage fluid of mice exposed to B20 were ~20–30% higher than control or B0 PM, suggesting that addition of biodiesel to diesel fuels will reduce PM emissions but not necessarily adverse health outcomes.

INTRODUCTION

Biodiesel, a renewable fuel derived from a variety of animal or vegetable fats, is a drop-in alternative to petroleum diesel. Since 2005, U.S. energy policy has mandated increases in the quantity of renewable fuels used for transportation, including “biomass-based diesel”.^{1–3} Hence, the expected increase in future use of biodiesel emphasizes the critical need to understand the health and environmental effects of biodiesel combustion. Data about the biological and health effects of biodiesel emissions are very limited and have stimulated debate about the pros and cons of changing fuel supplies.^{4–7} Comparing the results of different health effects studies for exhaust particles produced by biodiesel and petrodiesel combustion is difficult because of differences in the experimental methods used, including age and type of diesel engine, drive cycle, fuel feedstock, and percentage in the blended fuel. Early publications lack information on fuel composition and emissions sampling procedures.

*Corresponding author contact information: University of Vermont, Colchester Research Facility, 208 S. Park Dr., Room 173, Colchester, VT 05446, Phone: (802) 656-4403, Fax: (802) 656-2636, Naomi.Fukagawa@uvm.edu.

SUPPORTING INFORMATION AVAILABLE

Detailed chemical extraction and TD-GCMS analysis procedures, cell culture and biological assay techniques, and supplementary data are available free of charge via the internet at <http://pubs.acs.org/>.

Diesel engine emissions are an important source of particulate matter (PM) in ambient air and many occupational settings. New diesel engines have been engineered to yield lower regulated emissions (PM, CO, HC, NO_x), but exposure continues to pose adverse health risks due to increased ultrafine (particle diameter, D_p < 100 nm) and nanoparticle (D_p < 50 nm) emissions.^{5–7} The commercial biodiesel blend most commonly used in on-road vehicles in the U.S. is a 20% soybean biodiesel blend (B20; 20% biodiesel and 80% petrodiesel, by volume). Only recently has the detailed chemical composition of biodiesel exhaust PM been reported.^{8,9} Combustion of biodiesel compared to petrodiesel produced lower emissions of CO, hydrocarbons and PM mass,^{3,10} smaller diameter ultrafine particles, lower polycyclic aromatic hydrocarbons (PAH) and either lower or higher concentrations of gas-phase carbonyls, depending on the operating conditions of the engine and the composition of the biodiesel fuel.^{11–13} The mechanisms whereby particles affect health are believed to involve oxidative stress at the cellular level, either induced indirectly by the particles contributing to reactive oxygen species (ROS) production, or directly via ROS-bearing functionalities within the particles. A number of studies have quantified the “oxidative potential” of exhaust particles using an abiotic dithiothreitol (DTT) assay.^{14,15} While these abiotic tests are informative in a relative sense, they cannot account for the particle/cell interactions necessary for health-related outcomes. The more polar, water soluble organic carbon fraction of biodiesel PM has been associated with particle oxidative potential, and ROS increased as the percentage of biodiesel in the blend increased but there did not appear to be a significant effect of the feedstock.^{8,14} Other investigators have suggested that PM from biodiesel in equal mass concentrations was less toxic than conventional petrodiesel based on ROS production and DNA damage.⁵ However, a recent study reported that extracts from PM produced by combustion of a 50% rapeseed blend (B50) by Euro 4 light-duty passenger cars resulted in increased cytotoxicity and IL-6 release by bronchial epithelial cells (BEAS-2B).¹⁶

The objective of this work was to: (1) characterize exhaust particles produced by combustion of pure petrodiesel (B0) and B20 fuels using the same engine and running conditions; (2) compare the *in vitro* responses of BEAS-2B and macrophages (differentiated THP-1 monocytes) after 24 h of exposure to PM; and (3) evaluate the *in vivo* responses of mice receiving the same particles by oropharyngeal aspiration for 3 consecutive days. Concentrations of inflammatory mediators, cytotoxicity and formation of ROS and oxidation products were measured in cell cultures exposed to B0 and B20 at two particle concentrations. We then examined the *in vivo* responses to the same particles in mice as the next step towards elucidating potential health effects.

MATERIALS AND METHODS

(See Supporting information (SI) for details of procedures for extraction, TD-GCMS, cell/animal treatments and biological assays).

Exhaust Particle Generation and Collection

A 4-cylinder, 1.9 Liter Volkswagen light-duty diesel engine and Klam dynamometer (Armfield CM-12) were operated at various throttle and brake settings over a 9-mode steady-state cycle (SI Tables S1–S2) to enable triplicate time-resolved measurement of particle number distributions with a Scanning Mobility Particle Sizer (SMPS, TSI, Inc. Model 3080/3081 long DMA, 3025A UCPC; 120 s upscan, 30 s retrace). Particles for chemistry and gravimetric mass were collected on 47 mm side-by-side Teflon-coated glass fiber (Pall Gelman T60A20) and Teflo filters, and side-by-side 60 mL Teflon (Savillex; 30mL ethanol) impingers for *in vitro* and *in vivo* experiments. Filter samples were collected from raw exhaust without dilution, but SMPS particle distribution was measured after

single-stage dilution with HEPA-filtered, dry (silica gel) room air at a dilution ratio of ~20. After post-weighing, filter samples were stored at -80°C until chemical analysis by thermal desorption-gas chromatography mass spectrometry (TD-GCMS). Blank runs were performed identically without starting the diesel engine for 50 minutes. Filter and impinger samples were collected over 75-minute periods that did not include engine start and warm-up (defined by stable coolant temperature, 92°C).

Two fuel compositions, ultralow sulfur petrodiesel (Shell/Trono Fuels, Burlington, Vermont; "B0") and certified soy-based biodiesel (Patriot Fuels, Brockton, MA) blended at 20% by volume, were used. B20 was blended in the laboratory 24-hours prior to experiments, and the blend volume percent and presence of any impurities verified via Fourier transform infrared spectroscopy (FTIR) spectral analysis (Grabner Instruments IROX-D).

TD-GCMS

Particle composition was determined by thermal desorption (TD)-GCMS after extracting 1/4-inch diameter punches of the filters using hexane/dichloromethane followed by methanol in triplicate, concentration under N_2 gas, and addition of sample and deuterated phenanthrene internal standard into a TD borosilicate glass vial. The methanol extract was derivatized with pentafluorobenzyl hydroxylamine to quantify polar organic compounds. Polar and nonpolar compound identification was based on the NIST08 mass spectral library match for functional group comparisons of the filter extracts (SI). Individual compounds containing oxygen-bearing functional groups were quantified as "polar" (alcohols, aldehydes, acids, esters, ketones) assuming a response factor of 1 for all compounds. This enabled relative comparison of particle organic composition between the fuel types. Sixteen EPA priority PAHs were quantified using extracted ion calibration curves developed using authentic standards.

Preparation of Particle Stock Suspensions

Raw exhaust particles collected in ethanol impingers were concentrated via gentle N_2 blowdown to generate stock suspensions of approximately 1 mg/ml. PM concentrations of impinger suspensions were determined in triplicate using gravimetric analysis (Cahn C-31 microgram balance, 0.001 mg sensitivity) of 100 μL aliquots prepared prior to, during, and after dilution of the stock suspension with Milli-Q water to obtain aqueous solutions with final ethanol concentrations less than 10% v/v to avoid cell death.¹⁷

Abiotic Assays

Because PM may inherently induce oxidative stress, ROS production by the PM used in these experiments was examined with the DTT assay.¹⁴⁻¹⁶ Because PM may bind small proteins, such as cytokines, and affect concentration measurements, cytokine adsorption to PM was determined by treating particles with different cytokine concentrations and measuring levels of unbound cytokine in the medium.

In Vitro and *In Vivo* Particle Exposures

In vitro cell experiments were conducted with human THP-1 monocytes differentiated into macrophages with phorbol myristic acid (PMA) and BEAS-2B cells (ATCC, Manassas, VA). Cells seeded at 3×10^6 per 60 cm^2 were directly treated with the B0 or B20 engine exhaust particles at final concentrations of 10 and 20 $\mu\text{g}/\text{ml}$ and the same volume of 8% ethanol as the vehicle control (final ethanol concentration $<0.1\%$). Selected doses were comparable to those used in previous studies for petrodiesel.^{18,19} Amorphous silica and cristobalite (20 Pg/ml) were used as respirable particle controls, respectively, for the *in vitro*

experiments. Cristobalite is a crystalline silica that is potentially carcinogenic and associated with pneumoconiosis whereas amorphous silica, which does not have a specific crystalline structure, causes a transient inflammatory response without long-lasting lung pathology.²⁰ After 24 h of exposure, particles were removed by centrifugation followed by collection of culture medium and total protein from cell lysates for subsequent analyses.

In vivo experiments used female C57BL/6 mice (Jackson Laboratories, Bar Harbor, ME, n=6 per group) exposed to B20 and B0 particles (~84 µg/treatment) or vehicle control (50 µl 8% ethanol) administered via the oropharyngeal (OP) aspiration.²¹ Dose was based on previous petrodiesel studies.^{22–24} Mice were euthanized after 3 consecutive days of OP exposure and lungs were lavaged for evaluation of cell counts and biological measures as previously described.^{21,25} Protein was isolated from the right lung lobes using standard techniques. These experiments evaluated whether particles from the combustion of either fuel resulted in unique responses associated with development of pulmonary inflammation.

Biological Assays

Cell culture medium, animal bronchoalveolar lavage fluid (BALF) and lung tissue proteins were examined for inflammatory mediators and specific proteins related to disease pathogenesis. The outcome variables included indices of cell toxicity, inflammation, oxidative stress, and biomarkers of lung injury and antioxidant responses.

Data Analysis

Statistical analysis included ANOVA with Tukey's post-hoc comparisons using GraphPad 5 software. Comparisons were made between control and treated groups and post-hoc analysis for differences between the fuels. $P < 0.05$ was considered statistically significant.

RESULTS AND DISCUSSION

Engine Performance and Exhaust Particle Characterization

Overlap in the engine performance metrics for the 2 fuel types (data not shown) demonstrated that tests conducted on different days were quite similar. Recorded 1 Hz throttle, engine load, engine speed, and fuel consumption data over the 75-minute test period overlapped, confirming that the lower energy content of the biodiesel fuel had little effect on the ability of the engine to generate torque and follow the assigned drive cycle at the B20 blend level. Two B0 and four B20 runs were completed for characterization of PM emissions. A subset of the collected filter and impinger samples were used in detailed chemical composition and biological response experiments.

The total particulate gravimetric mass collected over the engine test cycle was more than 2 times higher for B0 than for B20 fuel combustion (Table 1). The lower B20 emissions are consistent with reported literature trends, but the magnitude in mass difference reflects collection of raw exhaust particle samples without dilution. The B20 PM concentrations showed higher variability compared to B0 (34% vs <1%) as expected for the higher semi-volatile organic carbon composition of biodiesel PM (see GCMS results below) and suggests variability introduced by gas/particle partitioning during sampling of undiluted exhaust. The undiluted filter samples were collected to enable chemical characterization of the same particles collected by impingers for use in biological experiments.

The IROX-Diesel properties for fuel samples collected from the engine's fuel tank after each emissions test confirmed the volume percent biodiesel in the B20 fuel was 19.6 (compared to 0.5 for the B0, indicating the instrument's error). The IROX-Diesel-measured fuel density

of B20 (0.829) was slightly higher than that for B0 (0.819), in agreement with literature trends³.

Particle number distributions (Figure 1) computed as averages in each SMPS size bin (~6 to 250 nm diameter range) aggregated over one example drive cycle indicate a unimodal B0 distribution centered at 51 nm, but a B20 distribution with a smaller diameter mode at 32.2 nm and a shoulder that corresponded to the B0 peak at ~51 nm. The formation of smaller nanoparticles for B20 compared to the baseline B0 agrees with recent literature.⁸ The error bars in Figure 1 show more variability for the B20 fuel, an observation consistent with the gravimetric mass data and the sensitivity of particle distributions to gas/particle partitioning and particle nucleation during sampling.²⁶ Surface areas computed from the SMPS number distributions showed that total integrated surface area of B20 particles was 2 times higher than that for B0 particles (SI Figure S1). More refined analysis of the SMPS scans on individual brake/throttle settings determined that these smaller B20 particles formed during all but one operating mode (SI Figure S2).

B0 particles were chiefly nonpolar and included n-alkanes, alkenes and 16 identified PAHs, representing ~68% of the identified mass (Figure 2). About 46% of the B0 PM was comprised of polar compounds, chiefly esters, ketones and acids, in agreement with previous studies.²⁷ Similar n-alkane and Unresolved Complex Mixture (UCM) patterns were observed for the B20 PM, as expected because the same petrodiesel base fuel was used to prepare the B20 blend. In addition, fatty acid methyl esters (FAME), reflecting composition of the original soy feedstock for the pure biodiesel, were detected in the B20 particles. The relative percentages of palmitate, stearate, oleate, linoleate and linolenate fatty acid methyl esters quantified in the B20 PM (12, 14, 61, 11 and 2%, respectively) were shifted from published soybean oil compositions (10–12%, 3–5%, 18–26%, 49–57% and 6–9%, respectively),²⁸ due to oxidation of longer chain FAME during combustion. The original fuel was not analyzed by GCMS. These data suggest more information is needed on the shorter chain FAME that form during FAME combustion, given that palmitic, oleic and stearic acids are known pulmonary irritants.²⁹

The most significant compositional difference between the exhaust PM from combustion of the 2 fuels was the ratio of polar to nonpolar species: 46% assigned polar for B0 vs. 68% polar compounds for the B20 fuel (Figure 2). We are unaware of previous studies reporting this type of comparison of the exhaust PM. However, our results are qualitatively consistent with previous work reporting lower elemental-to-organic carbon (EC/OC) ratio of biodiesel vs. petrodiesel exhaust PM.^{8,14} Biodiesel PM contains a higher proportion of water-soluble organic carbon relative to petrodiesel PM. Addition of 20% soy biodiesel to B0 reduced the total PAH mass concentration by a factor of 2 for the 16 PAHs quantified with authentic standards. Benzo(a)pyrene, an IARC Class I carcinogen, was 2 times higher in B0 exhaust compared to B20 (SI Table S3), a result consistent with one previous study on rapeseed B30.³⁰

***In Vitro* and *In Vivo* Responses to PM**

No significant cytotoxicity was found in the BEAS-2B and THP-1 cell lines after treatment with PM from either fuel at the two concentrations tested (SI Figure S5). In contrast and as expected, cristobalite was cytotoxic in BEAS-2B cells.

THP-1 cells, representing macrophages that are one of the first lines of defense after particle exposure, responded with increases in several inflammatory mediators, including granulocyte colony stimulating factor (G-CSF), Interleukin (IL)-8 and Tumor necrosis factor-alpha (TNF- α) (Figure 3A). B20 particles elicited a higher mean response than cristobalite, amorphous silica and B0 particles although values were variable. Of interest but

for unclear reasons, the lower (10 µg/ml) dose of B20 particles (B20-10) consistently elicited a higher response than the 20 µg/ml dose (B20-20). BEAS-2B cells, representing the lung epithelium, secreted significantly higher levels of IL-8 in B20-20 compared to B0-20. Concentrations of Monocyte-chemoattractant Protein-1 (MCP-1) were higher in B20-10, B0-10 and B0-20 compared to vehicle and other treatments (Figure 3B). SI Tables S4 and S5 show the results for the other cytokines/chemokines that were detectable in the assay used. The variable patterns in both cell types have been previously reported⁵ and are likely attributable to different experimental conditions, including engine technology and operation, fuel type, nature of particles tested (concentration or sample preparation as suspensions or extracts)^{7,16}.

Although carbonaceous PM, like diesel exhaust, may adsorb small proteins such as cytokines^{31–33} and potentially affect the accuracy of the cytokine assay, no significant decrease in G-CSF was detected in a cell-free system containing only cytokines at concentrations of 100–400 pg/ml for G-CSF and particles at 0–40 µg/ml (SI Figure S6).

In vivo responses to aspiration of PM were determined in samples of BALF and lung tissue. Particles from both fuels elicited an increase in total cell counts ($\times 10^4$) in BALF but there was no significant difference in the magnitude of effects of the 2 fuels. The types of cells in the BALF were significantly different compared to control but similar between the fuels (Table 2), as previously reported^{34,46}.

Five BALF cytokines (G-CSF, IL-5, IL-6, IP-10 and KC) were interpretable with the cytokine/chemokine assay; three of which were significantly higher in B20-exposed mice than both control- and B0-exposed animals (Figure 4A). KC, one of the murine IL-8 homologues, and IL-5 results are shown in SI Table S6A.

Cytokines measured in lung homogenates confirmed the significant increases in G-CSF, IP-10, and IL-6 in the BALF of B20-exposed mice (Figure 4B). Lung KC, MCP-1, and IL-13 levels appeared slightly increased in the B20 group as shown in SI Table S6B, but results did not achieve statistical significance. Overall, these findings are generally consistent with previous reports^{5,34,46} although the magnitude of the response and specific cytokines may differ.

Together, *in vitro* and *in vivo* cytokine/chemokine data demonstrate an induction of inflammation as a consequence of exposure to the same mass concentrations of PM from B20 and B0 combustion with a higher response to B20 than B0, implying that acute exposure to biodiesel exhaust may be associated with more significant health outcomes. To determine the possible mechanism for the responses to PM, indices of oxidative stress and antioxidant defense were assessed.

Oxidative Stress and Antioxidant Defense

The DTT assay to assess ROS associated with PM resulted in increased DTT consumption. After 45-minute incubation, DTT was significantly consumed by B20 (30%) compared to the same mass of B0 (21%) shown in Figure 5A. The OxySelect ROS Assay (Figure 5B) showed that all the treatments, including B20 and B0, induced ROS formation significantly at 1 and 2 hours. After 24 hours of exposure to either exhaust PM, cellular ROS returned to control levels suggesting that both B20 and B0 PM can produce immediate but not long-lasting intracellular ROS. No ROS effects were found with treatment of BEAS-2B cells (data not shown). ROS were not directly measured *in vivo* but determination of protein carbonyls as an index of oxidized protein in the lung homogenates was consistent with greater oxidative stress after exposure to B20 than control (Figure 5C). A representative

OxyBLOT on the right shows more multiple dark bands indicative of protein oxidation in B20 compared to B0.

To assess antioxidant defenses in the animals, Western blot analysis of lung homogenates revealed increased catalytic subunit of glutamate-cysteine ligase (GCLC), the enzyme catalyzing the rate-limiting step in the synthesis of glutathione (GSH), the body's major endogenous antioxidant, in mice treated with B20 PM ($p < 0.05$) compared to the control (Figure 5D, right panel). Consistent with the GCLC increase, there was a slight but insignificant increase in Nrf2, a transcription factor involved in the regulation of GCLC, in B20-treated but not in B0-treated animals (Figure 5D, left panel). Furthermore, lower levels of total GSH in blood were seen in both B20- and B0-treated mice (Figure 5E), consistent with the increased protein carbonyls and upregulation of the Nrf2-GCLC pathway.

Another biomarker affected in the lung is plasminogen activator inhibitor-1 (PAI-1), a key component of the fibrinolytic system and expressed by lung epithelial cells.³⁵ PAI-1 has been implicated in the pathogenesis of acute lung injury and pulmonary fibrosis.³⁶⁻³⁸ Increased PAI-1 is closely linked to inflammation,^{39,40} oxidative stress,^{41,42} and pro-coagulation.^{43,44} To determine whether PAI-1 expression was changed with *in vivo* animal exposures, PAI-1 concentrations in BALF were measured (SI Figure S7A). Compared to controls, PAI-1 increased in the BALF of mice exposed to both B0 and B20 PM to a similar magnitude for both fuels. PAI-1 protein was also detectable in lung homogenates, but there was no significant effect of the 2 particle types (SI Figure S7B), perhaps because lung homogenates represent a variety of cell types that differ in their PAI-1 responses. These findings suggest that PM induces PAI-1 but, unlike the inflammatory cytokines/chemokines, the increases were not related to the type of fuel.

Taken together with the findings on particle characterization, it appears that the greater inflammatory responses and ROS production seen in cells and animals treated with B20 compared to B0 may be linked to the large polar component in B20 exhaust. Addition of 20% FAMES to the base B0 changed the combustion products significantly as indicated in Figure 2. However, the relative speciation profiles reported here are not sufficient for complete mechanistic understanding of the inflammatory responses. As reported by Jalava et al. using a heavy-duty EURO IV diesel engine, a conventional diesel fuel (EN590) and 2 biodiesel fuels (rapeseed methyl esters, RME, and hydrotreated vegetable oil, HVO), both biofuels produced lower PAH and smaller mass⁴⁵. However, pure HVO and RME induced stronger ROS production and HVO + catalyst induced the highest MIP-2 responses in a macrophage cell line RAW 264.7.⁴⁵ Other investigators found greater proinflammatory responses in BEAS-2B cells exposed to soy ethyl ester and soy methyl ester biodiesel compared to petrodiesel⁶. In a study to assess cardiovascular and inflammatory toxicity of petrodiesel and biodiesel particles by measuring a series of symptoms and biomarkers, investigators concluded that biodiesel was more toxic than petrodiesel because it promoted functional cardiovascular alterations although the responses in pulmonary and systemic inflammation were similar between fuel types.⁴⁵ More recently, Yanamala et al reported that biomarkers of lung injury and inflammation were consistent with greater toxicity of biodiesel compared to petrodiesel exhaust⁴⁶. There appears to be some consensus that the chemical composition of biodiesel PM is responsible: Petrodiesel emissions contain substantially more total PAHs than rapeseed oil emissions, while carcinogenic PAH (c-PAH) levels were comparable or significantly higher for rapeseed oil emissions^{8,10,30,45}. Furthermore, although biodiesel is promoted as being environmentally less harmful than petrodiesel, its water-soluble-fraction may contain methanol, which appears by a reversion of the transesterification reaction when biodiesel contacts water.⁴⁷ More ultrafine particles (UFPs, <100nm) were emitted when an engine was fueled with waste cooking oil biodiesel, and UFPs contributed a major fraction (>70%) of the total estimated health risk.⁴⁸ Hence,

although B20 produced less particle mass than B0, the relative smaller size but higher surface area, more polar components and FAME of B20 particles may contribute to greater biological effects per mass than B0, leading to potentially greater health risks.

For the data reported here, the same procedures were used for the two fuel types with the assumption that similar changes in particle morphology would occur during handling, but differences in aqueous solubility may have affected the final delivery dose in the experiments. Future work is clearly needed to more thoroughly characterize the exhaust particles from biodiesel combustion under a wide range of engine operating conditions so that the real-world health effects of fuel switching can be quantified.

Supplementary Material

Refer to Web version on PubMed Central for supplementary material.

Acknowledgments

This study was supported by NIH/NIEHS grants R03ES017860-01 and RC1-ES018053-01 (ARRA Challenge). We thank Vaishali Sharma and Brad Haire for experimental assistance, Tyler Feralio for engine emissions testing assistance, Philip Cannata for GCMS data analysis, and Rebecca Aksdal for editorial assistance.

References

1. U.S.Congress *Energy independence and security act of 2007; Jan 4, 2007; 110th Congress, First Session, H.R. 6; 07.*
2. U.S.Environmental Protection Agency. US EPA Finalizes 2011 Renewable Fuel Standards. U.S. EPA Office of Transportation and Air Quality; Ann Arbor, MI: 2013. p. 3
3. U.S.Environmental Protection Agency. A comprehensive analysis of biodiesel impacts on exhaust emissions. 2002. EPA420-P-02-001
4. Krahl J, Munack A, Schroder O, Stein H, Bunger J. Influence of biodiesel and different designed diesel fuels on the exhaust gas emissions and health effects 2003-01-3199. Society of Automotive Engineers. 03
5. Hemmingsen J, Moller P, Nojgaard J, Roursgaard M, Loft S. Oxidative stress, genotoxicity, and vascular cell adhesion molecule expression in cells exposed to particulate matter from combustion of conventional diesel and methyl ester biodiesel blends. *Environ Sci Technol.* 2011; 45(19):8545-8. [PubMed: 21842833]
6. Swanson KJ, Funk WE, Pleil JD. Release of the pro-inflammatory markers by BEAS-2B cells following in vitro exposure to biodiesel extracts. *The Open Toxicology Journal.* 2009; 3:8-15.
7. Jalava PI, Tapanainen M, Kuusalo K, Markkanen A, Hakulinen P, Happonen MS, Pennanen AS, Ihalainen M, Yli-Pirila P, Makkonen U, Teinila K, Maki-Paakkanen J, Salonen RO, Jokiniemi J, Hirvonen MR. Toxicological effects of emission particles from fossil- and biodiesel-fueled diesel engine with and without DOC/POC catalytic converter. *Inhal Toxicol.* 2010; 22(Suppl 2):48-58. [PubMed: 21029031]
8. Surawski NC, Miljevic B, Ayoko GA, Elbagir S, Stevanovic S, Fairfull-Smith KE, Bottle SE, Ristovski ZD. Physicochemical Characterization of Particulate Emissions from a Compression Ignition Engine: The Influence of Biodiesel Feedstock. *Environmental Science & Technology.* 2011; 45(24):10337-10343. [PubMed: 22039912]
9. Surawski NC, Miljevic B, Ayoko GA, Roberts BA, Elbagir S, Fairfull-Smith KE, Bottle SE, Ristovski ZD. Physicochemical Characterization of Particulate Emissions from a Compression Ignition Engine Employing Two Injection Technologies and Three Fuels. *Environmental Science & Technology.* 2011; 45(13):5498-5505. [PubMed: 21627159]
10. Durbin TD, Collins JR, Norbeck JM, Smith MR. Effects of biodiesel, biodiesel blends, and a synthetic diesel on emissions from light heavy-duty diesel vehicles. *Environmental Science & Technology.* 2000; 34(3):349-355.

11. Peng C-Y, Yang H-H, Lan C-H, Chien SM. Effects of the biodiesel blend fuel on aldehyde emissions from diesel engine exhaust. *Atmospheric Environment*. 2008; 42(5):906–915.
12. Lapuerta M, Rodriguez-Fernandez J, Agudelo JR. Diesel particulate emissions from used cooking oil biodiesel. *Bioresource Technology*. 2008; 99(4):731–740. [PubMed: 17368887]
13. Karavalakis G, Boutsika V, Stournas S, Bakeas E. Biodiesel emissions profile in modern diesel vehicles. Part 2: Effect of biodiesel origin on carbonyl, PAH, nitro-PAH and oxy-PAH emissions. *Science of The Total Environment*. 2011; 409(4):738–747. [PubMed: 21122895]
14. Biswas S, Verma V, Schauer JJ, Cassee FR, Cho AK, Sioutas C. Oxidative potential of semi-volatile and non volatile particulate matter (PM) from heavy-duty vehicles retrofitted with emission control technologies. *Environ Sci Technol*. 2009; 43(10):3905–3912. [PubMed: 19544906]
15. Cheung KL, Polidori A, Ntziachristos L, Tzankiozis T, Samaras Z, Cassee FR, Gerlofs M, Sioutas C. Chemical characteristics and oxidative potential of particulate matter emissions from gasoline, diesel, and biodiesel cars. *Environ Sci Technol*. 2009; 43(16):6334–6340. [PubMed: 19746734]
16. Gerlofs-Nijland ME, Totlandsdal AI, Tzankiozis T, Leseman DL, Samaras Z, Lag M, Schwarze P, Ntziachristos L, Cassee FR. Cell toxicity and oxidative potential of engine exhaust particles: impact of using particulate filter or biodiesel fuel blend. *Environ Sci Technol*. 2013; 47(11):5931–5938. [PubMed: 23597117]
17. Castilla R, Gonzalez R, Fouad D, Fraga E, Muntane J. Dual effect of ethanol on cell death in primary culture of human and rat hepatocytes. *Alcohol Alcohol*. 2004; 39(4):290–296. [PubMed: 15208159]
18. Nam HY, Ahn EK, Kim HJ, Lim Y, Lee CB, Lee KY, Vallyathan V. Diesel exhaust particles increase IL-1beta-induced human beta-defensin expression via NF-kappaB-mediated pathway in human lung epithelial cells. *Part Fibre Toxicol*. 2006; 3:9. [PubMed: 16723032]
19. Xiao GG, Wang M, Li N, Loo JA, Nel AE. Use of proteomics to demonstrate a hierarchical oxidative stress response to diesel exhaust particle chemicals in a macrophage cell line. *J Biol Chem*. 2003; 278(50):50781–50790. [PubMed: 14522998]
20. Perkins TN, Shukla A, Peeters PM, Steinbacher JL, Landry CC, Lathrop SA, Steele C, Reynaert NL, Wouters EF, Mossman BT. Differences in gene expression cytokine production by crystalline vs amorphous silica in human lung epithelial cells. *Part Fibre Toxicol*. 2012; 9(1):6. [PubMed: 22300531]
21. Lakatos HF, Burgess HA, Thatcher TH, Redonnet MR, Hernady E, Williams JP, Sime PJ. OROPHARYNGEAL ASPIRATION OF A SILICA SUSPENSION PRODUCES A SUPERIOR MODEL OF SILICOSIS IN THE MOUSE WHEN COMPARED TO INTRATRACHEAL INSTILLATION. *Experimental Lung Research*. 2006; 32(5):181–199. [PubMed: 16908446]
22. Lewis JA, Rao KM, Castranova V, Vallyathan V, Dennis WE, Knechtges PL. Proteomic analysis of bronchoalveolar lavage fluid: effect of acute exposure to diesel exhaust particles in rats. *Environ Health Perspect*. 2007; 115(5):756–763. [PubMed: 17520064]
23. Yoshizaki K, Brito JM, Toledo AC, Nakagawa NK, Piccin VS, Junqueira MS, Negri EM, Carvalho AL, Oliveira AP, Lima WT, Saldiva PH, Mauad T, Macchione M. Subchronic effects of nasally instilled diesel exhaust particulates on the nasal and airway epithelia in mice. *Inhal Toxicol*. 2010; 22(7):610–617. [PubMed: 20429853]
24. Nemmar A, Al Salam S, Dhanasekaran S, Sudhadevi M, Ali BH. Pulmonary exposure to diesel exhaust particles promotes cerebral microvessel thrombosis: Protective effect of a cysteine prodrug 1-2-oxothiazolidine-4-carboxylic acid. *Toxicology*. 2009; 263(2–3):84–92. [PubMed: 19560508]
25. Fukagawa NK, Li M, Sabo-Attwood T, Timblin CR, Butnor KJ, Gagne J, Steele C, Taatjes DJ, Huber S, Mossman BT. Inhaled asbestos exacerbates atherosclerosis in ApoE-deficient mice via CD4+ T cells. *Environmental Health Perspectives*. 2008; 116(9):1218–1225. [PubMed: 18795166]
26. Kittelson DB. Engines and nanoparticles: A review. *Journal of Aerosol Science*. 1998; 29(5–6): 575–588.
27. Schauer JJ, Kleeman MJ, Cass GR, Simoneit BRT. Measurement of emissions from air pollution sources 2 C1–C30 organic compounds from medium duty diesel trucks. *Environmental Science & Technology*. 1999; 33(10):1578–1.

28. Knothe G. "Designer" biodiesel: Optimizing fatty ester composition to improve fuel properties. *Energy & Fuels*. 2008; 22:1358–1364.
29. Madden, MC.; Bhavaraju, L.; Kodavant, UP. Toxicology of biodiesel combustion products. In: Montero, G.; Stoytcheva, M., editors. *Biodiesel-Quality, Emissions, and By-products*. 2011. p. 195-214. InTechWeb Org
30. Macor A, Avella F, Faedo D. Effects of 30% v/v biodiesel/diesel fuel blend on regulated and unregulated pollutant emissions from diesel engines. *Applied Energy*. 2011; 88(12):4989–5001.
31. Brown DM, Dickson C, Duncan P, Al-Attili F, Stone V. Interaction between nanoparticles and cytokine proteins: impact on protein and particle functionality. *Nanotechnology*. 2010; 21(21): 215104. [PubMed: 20431193]
32. Howell CA, Sandeman SR, Phillips GJ, Lloyd AW, Davies JG, Mikhalovsky SV, Tennison SR, Rawlinson AP, Kozynchenko OP, Owen HL, Gaylor JD, Rouse JJ, Courtney JM. The in vitro adsorption of cytokines by polymer-pyrolysed carbon. *Biomaterials*. 2006; 27(30):5286–5291. [PubMed: 16806458]
33. Kocbach A, Totlandsdal AI, Låg M, Refsnes M, Schwarze PE. Differential binding of cytokines to environmentally relevant particles: A possible source for misinterpretation of in vitro results? *Toxicology Letters*. 2008; 176(2):131–137. [PubMed: 18079072]
34. Brito JM, Belotti L, Toledo AC, Antonangelo L, Silva FS, Alvim DS, Andre PA, Saldiva PH, Rivero DH. Acute cardiovascular and inflammatory toxicity induced by inhalation of diesel and biodiesel exhaust particles. *Toxicol Sci*. 2010; 116(1):67–78. [PubMed: 20385657]
35. Shetty S, Padijnayaveetil J, Tucker T, Stankowska D, Idell S. The fibrinolytic system and the regulation of lung epithelial cell proteolysis, signaling, and cellular viability. *Am J Physiol Lung Cell Mol Physiol*. 2008; 295(6):L967–L975. [PubMed: 18836029]
36. Courey AJ, Horowitz JC, Kim KK, Koh TJ, Novak ML, Subbotina N, Warnock M, Xue B, Cunningham AK, Lin Y, Goldklang MP, Simon RH, Lawrence DA, Sisson TH. The vitronectin-binding function of PAI-1 exacerbates lung fibrosis in mice. *Blood*. 2011; 118(8):2313–2321. [PubMed: 21734232]
37. Katre A, Ballinger C, Akhter H, Fanucchi M, Kim DK, Postlethwait E, Liu RM. Increased transforming growth factor beta 1 expression mediates ozone-induced airway fibrosis in mice. *Inhalation Toxicology*. 2011; 23(8):486–494. [PubMed: 21689010]
38. Senoo T, Hattori N, Tanimoto T, Furonaka M, Ishikawa N, Fujitaka K, Haruta Y, Murai H, Yokoyama A, Kohno N. Suppression of plasminogen activator inhibitor-1 by RNA interference attenuates pulmonary fibrosis. *Thorax*. 2010; 65(4):334–340. [PubMed: 20388759]
39. Xu X, Wang H, Wang Z, Xiao W. Plasminogen activator inhibitor-1 promotes inflammatory process induced by cigarette smoke extraction or lipopolysaccharides in alveolar epithelial cells. *Exp Lung Res*. 2009; 35(9):795–805. [PubMed: 19916862]
40. Budinger GRS, McKell JL, Urich D, Foiles N, Weiss I, Chiarella SE, Gonzalez A, Soberanes S, Ghio AJ, Nigdelioglu R, Mutlu EA, Radigan KA, Green D, Kwaan HC, Mutlu GkM. Particulate Matter-Induced Lung Inflammation Increases Systemic Levels of PAI-1 and Activates Coagulation Through Distinct Mechanisms. *PLoS ONE*. 2011; 6(4):e18525. [PubMed: 21494547]
41. Liu RM. Oxidative Stress, Plasminogen Activator Inhibitor 1, and Lung Fibrosis. *Antioxidants & Redox Signaling*. 2007; 10(2):303–320. [PubMed: 17979497]
42. Liu RM, Choi J, Wu JH, Gaston Pravia KA, Lewis KM, Brand JD, Mochel NS, Krzywanski DM, Lambeth JD, Hagood JS, Forman HJ, Thannickal VJ, Postlethwait EM. Oxidative modification of nuclear mitogen-activated protein kinase phosphatase 1 is involved in transforming growth factor beta1-induced expression of plasminogen activator inhibitor 1 in fibroblasts. *J Biol Chem*. 2010; 285(21):16239–16247. [PubMed: 20228065]
43. Kilinc E, Schulz H, Kuiper GJ, Spronk HM, Ten CH, Upadhyay S, Ganguly K, Stoeger T, Semmler-Bhenke M, Takenaka S, Kreyling WG, Pitz M, Reitmeier P, Peters A, Eickelberg O, Wichmann HE. The procoagulant effects of fine particulate matter in vivo. *Part Fibre Toxicol*. 2011; 8:12. [PubMed: 21406084]
44. Chuang KJ, Chan CC, Su TC, Lee CT, Tang CS. The effect of urban air pollution on inflammation, oxidative stress, coagulation, and autonomic dysfunction in young adults. *Am J Respir Crit Care Med*. 2007; 176(4):370–376. [PubMed: 17463411]

45. Jalava PI, Aakko-Saksa P, Murtonen T, Happonen MS, Markkanen A, Yli-Pirila P, Hakulinen P, Hillamo R, Maki-Paakkanen J, Salonen RO, Jokiniemi J, Hirvonen MR. Toxicological properties of emission particles from heavy duty engines powered by conventional and bio-based diesel fuels and compressed natural gas. *Part Fibre Toxicol.* 2012; 9:37. [PubMed: 23021308]
46. Yanamala N, Hatfield MK, Farcas MT, Schwegler-Berry D, Hummer JA, Shurin MR, Birch ME, Gutkin DW, Kisin E, Kagan VE, Bugarski AD, Shvedova AA. Biodiesel versus diesel exposure: Enhanced pulmonary inflammation, oxidative stress, and differential morphological changes in the mouse lung. *Toxicol Appl Pharmacol.* 2013; 272(2):373–383. [PubMed: 23886933]
47. da Cruz AC, Leite MB, Rodrigues LE, Nascimento IA. Estimation of biodiesel cytotoxicity by using acid phosphatase as a biomarker of lysosomal integrity. *Bull Environ Contam Toxicol.* 2012; 89(2):219–224. [PubMed: 22717620]
48. Betha R, Balasubramanian R. Emissions of particulate-bound elements from biodiesel and ultra low sulfur diesel: Size distribution and risk assessment. *Chemosphere.* 2013; 90(3):1005–1015. [PubMed: 22925425]

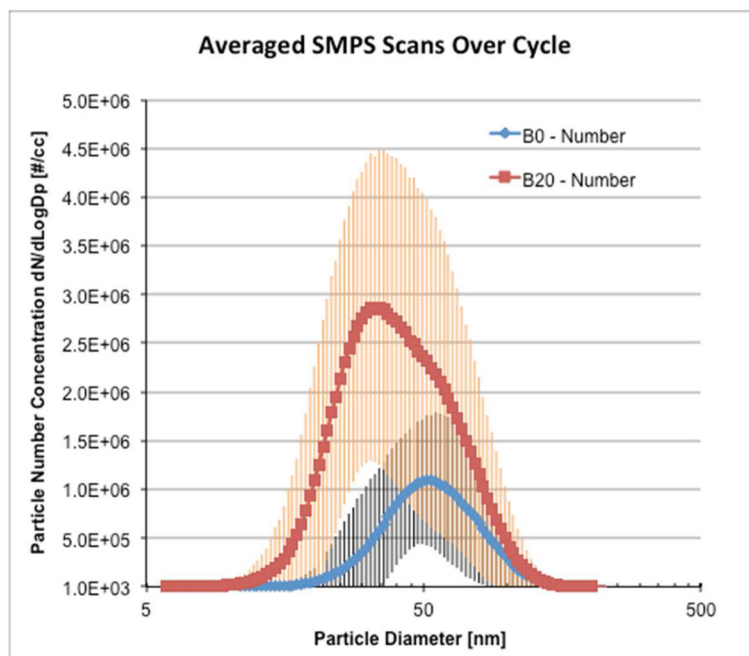


Figure 1. Mean particle number distributions for full cycle operation on petrodiesel (B0) and 20% soy biodiesel (B20) fuel. Error bars show one standard deviation over the test cycle.

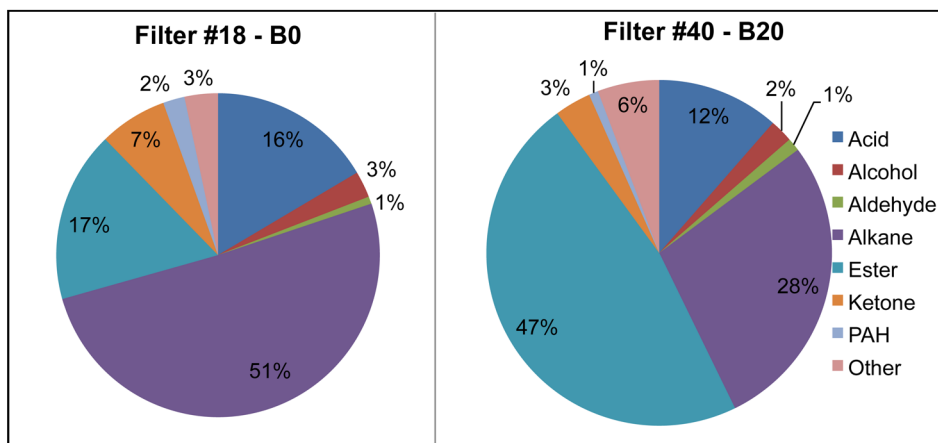
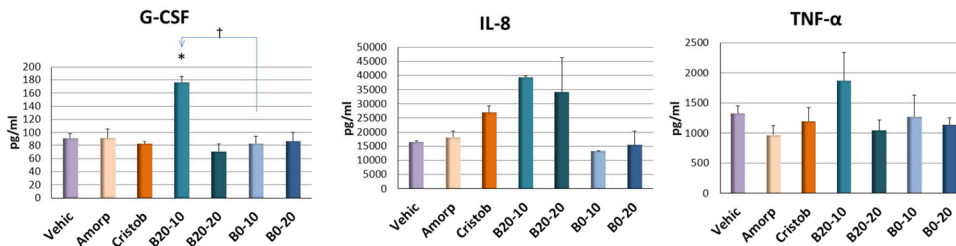


Figure 2.
Organic functional group composition of raw exhaust particles collected on filters.

A. Cytokines in THP-1 Cells



B. Cytokines in BEAS-2B-Cells

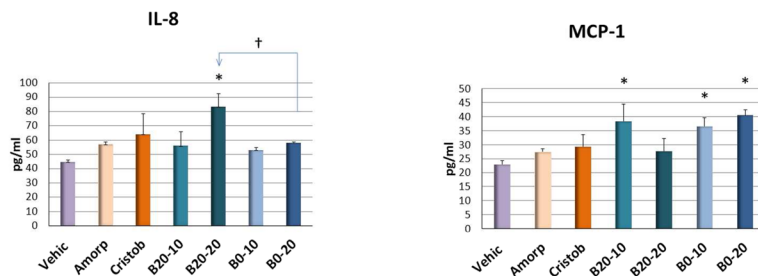
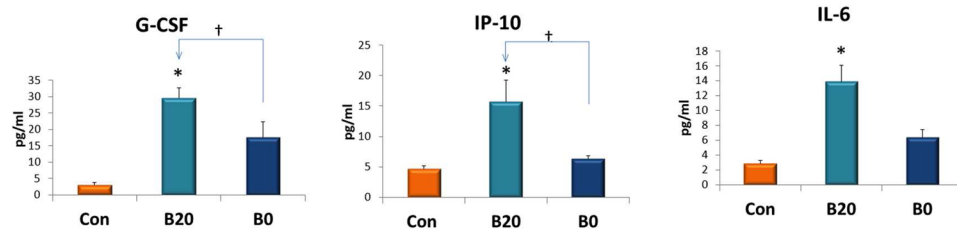
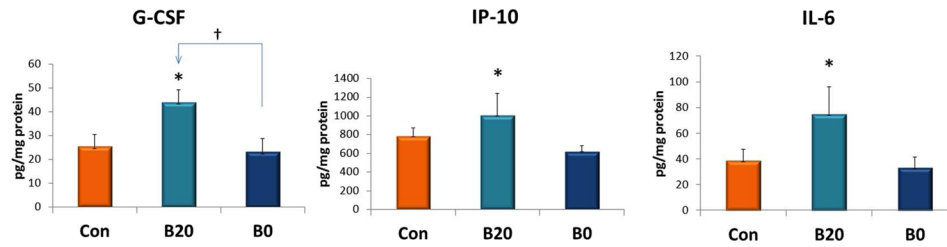


Figure 3. Selected cytokine/chemokine concentrations (mean±SE) in the medium of B0- and B20-treated THP-1 (A) and BEAS-2B cells (B). Vehicle control was 0.1% ethanol. 20 μg/ml Amorphous Silica (Amorp) and Cristobalite (Cristob) were used as respirable particle controls. Two doses of B20 and B0 (B20-10, 10 μg/ml; B20-20, 20 μg/ml; B0-10, 10 μg/ml; B0-20, 20 μg/ml) were used for treatments. Comparisons were only made between B20 and B0 with vehicle control (*P<0.05); or between the same concentration of B20 and B0 († P<0.05).

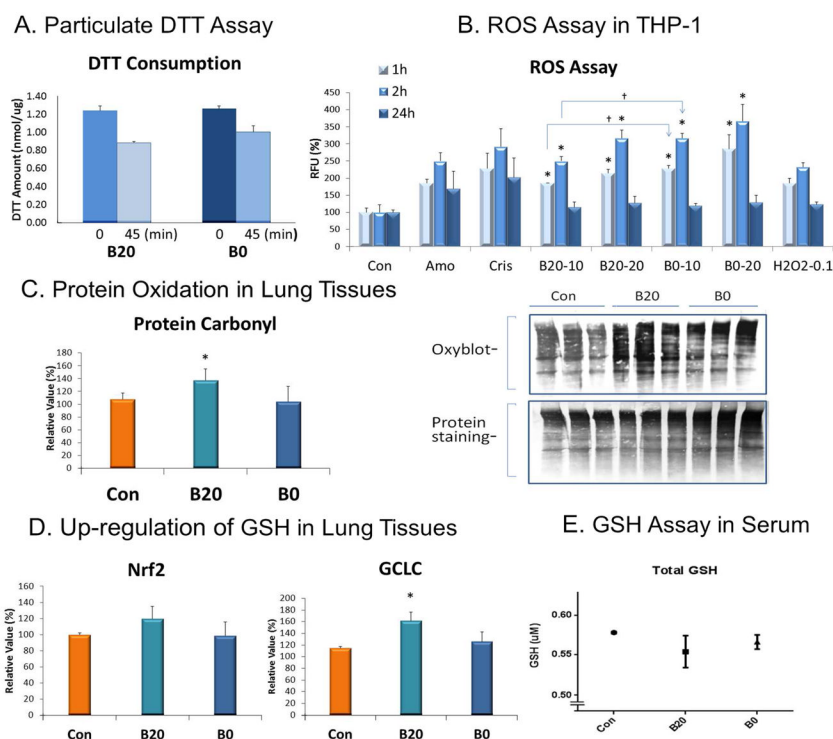
A. Cytokines in BALF



B. Cytokines in Lung Tissues

**Figure 4.**

Cytokine/chemokine concentrations (mean±SE) in bronchoalveolar lavage fluid (A) and lung tissue (B) from animals (n=5) exposed to B0 and B20 via oropharyngeal aspiration for 3 consecutive days. *P<0.05 compared to Control (Con: 8% ethanol); † P<0.05, B20 vs. B0.

**Figure 5.**

A. DTT consumption determined by measuring the concentration of the formation of 5-mercapto-2-nitrobenzoic acid using absorption at 412 nm and difference between the standard and sample. The data were collected at the initial (0) and end (45 min) timepoints and normalized to the quantity of particles (40 μg) in the incubation mixture. B. Both B20 and B0 particles elicited ROS formation in THP-1 cells. Intracellular ROS formation was measured after 1, 2 and 24 hours of particle exposure with the OxySelect ROS Assay. Comparisons were made between B20 and B0 with vehicle control (* $P < 0.05$) or between the same concentrations of B20 and B0 ($\dagger P < 0.05$). C. Protein oxidation detected with the OxyBLOT assay in protein extracted from lung tissue of mice exposed to B20 and B0. In the representative OxyBLOT ($n = 3$ mice/group), more multiple dark bands indicate more protein oxidation in B20. The bar graph summarizes data from 2 blots (* $P < 0.05$ compared to control, $n = 6$ per group). D. B20 up-regulated the Nrf2-GCLC pathway in the lung tissue. Right panel summarizes the Western blot results for GCLC expression in lungs (* $P < 0.05$ compared to control); Left panel summarizes the Western blot results for Nrf2, which is consistent with rise in GCLC. E. A trend towards lower total glutathione levels in serum measured by the OxiSelect™ Total Glutathione (GSSG/GSH) Assay is consistent with the increase in GCLC and Nrf2.

Table 1

Gravimetric PM mass results for raw exhaust filters by fuel type for 9-mode cycle*

	B0	B20
Number of replicate tests	2	4
Mean Mass collected (mg)	27.8	8.23
SD	0.5	2.8
CV (%)	1.7	34.1
PM concentration (mg/m ³)	28.3	8.4
SD	0.2	2.9
CV (%)	0.7	34.3

CV = coefficient of variation = ratio of standard deviation to mean, expressed as %.

Table 2

Total cell counts and distribution of cell types as percentage of total cells in BALF

Group	Total cell count (x 10 ⁴)	Macrophages	Lymphocytes	Neutrophils	Other
Con	06.2 ± 2.7	5.83 ± 1.0	0.11 ± 0.0	0.13 ± 0.0	0.08 ± 0.0
B20	15.7 ± 4.7*	15.47 ± 2.0*	0.26 ± 0.1*	1.12 ± 0.3*	0.29 ± 0.1*
B0	17.2 ± 5.7*	14.00 ± 1.9*	0.23 ± 0.1*	1.22 ± 0.2*	0.19 ± 0.1*

Values are mean ± SE (n=6 mice per group). Other includes primarily epithelial cells.

* p<0.01 compared to Control.